Human variation in gingival inflammation

Shatha Bamashmous[a,b,c], Georgios A. Kotsakis[d], Kristopher A. Kerns[a,b], Brian G. Leroux[b,e], Camille Zenobia[f], Dandan Chen[f], Harsh M. Trivedi[f], Jeffrey S. McLean[a,b,g,1], and Richard P. Darveau[a,b,g,1]

[a]Department of Periodontics, University of Washington, Seattle, WA 98195; [b]Department of Oral Health Sciences, University of Washington, Seattle, WA 98195; [c]Department of Periodontology, Faculty of Dentistry, King Abdulaziz University, 21589 Jeddah, Saudi Arabia; [d]Department of Periodontics, University of Texas Health Science Center, San Antonio, TX 78229; [e]Department of Biostatistics, University of Washington, Seattle, WA 98195; [f]Department of Oral Health Research, Colgate Palmolive Company, Piscataway, NJ 08854; and [g]Department of Microbiology, University of Washington, Seattle, WA 98195

Edited by Daniel A. Portnoy, University of California, Berkeley, CA, and approved May 28, 2021 (received for review February 19, 2021)

Oral commensal bacteria actively participate with gingival tissue to maintain healthy neutrophil surveillance and normal tissue and bone turnover processes. Disruption of this homeostatic host–bacteria relationship occurs during experimental gingivitis studies where it has been clearly established that increases in the bacterial burden increase gingival inflammation. Here, we show that experimental gingivitis resulted in three unique clinical inflammatory phenotypes (high, low, and slow) and reveal that interleukin-1β, a reported major gingivitis-associated inflammatory mediator, was not associated with clinical gingival inflammation in the slow response group. In addition, significantly higher levels of *Streptococcus* spp. were also unique to this group. The low clinical response group was characterized by low concentrations of host mediators, despite similar bacterial accumulation and compositional characteristics as the high clinical response group. Neutrophil and bone activation modulators were down-regulated in all response groups, revealing novel tissue and bone protective responses during gingival inflammation. These alterations in chemokine and microbial composition responses during experimental gingivitis reveal a previously uncharacterized variation in the human host response to a disruption in gingival homeostasis. Understanding this human variation in gingival inflammation may facilitate the identification of periodontitis-susceptible individuals. Overall, this study underscores the variability in host responses in the human population arising from variations in host immune profiles (low responders) and microbial community maturation (slow responders) that may impact clinical outcomes in terms of destructive inflammation.

gingivitis | periodontitis | chemokine | inflammation | oral microbiome

The stability in host–microbial interface is essential for health across mucosal surfaces in the human body. Barrier immunity is not characterized by the absence of bacteria but by their regulated presence under healthy immune surveillance. This has also been termed the parainflammatory state and is required for tissues to respond to insult and restore homeostasis (1–3). This is especially relevant on mucosal surfaces where there is a constant microbial challenge to the host immune system (4). For example, in oral mucosal surfaces, one of the main protective mechanisms of tissue, and therefore host protection from unwanted microbial colonization, is the constant highly orchestrated transit of neutrophils from the local periodontal vasculature through healthy gingival tissue and into the gingival crevice (5). There, neutrophil surveillance is essential for maintaining the proper amount and composition of dental plaque (6), a highly evolved and organized bacterial consortium found on the tooth surface that actively contributes to normal periodontal tissue function (5, 7). Studies in germ-free mice have revealed that dental plaque is essential for proper neutrophil homing (8–10) and also contributes to normal alveolar bone turnover processes (11, 12). Proper neutrophil monitoring of the dental plaque microbial biofilm therefore results in a process termed "healthy homeostasis," with the consequence being both 1) colonization resistant, a microbial protection mechanism that resists infection, as well as 2) maintaining the appropriate microbial composition for normal periodontal bone and tissue function (13).

Accumulation of dental plaque in the human-induced gingivitis experimental model is a convenient and reproducible model facilitating the study of the disruption of healthy tissue homeostasis (14, 15). The human experimental gingivitis model offers the unique advantage of monitoring disease development in real time in order to study the change from a healthy to dysbiotic state in human tissue. Studies employing this model have revealed rapid alterations in clinical measures of inflammation that parallel microbial plaque biomass increases and compositional changes during the development of gingivitis (16, 17). Furthermore, it has been reported that in human experimental gingivitis studies the subject-based susceptibility to plaque-induced gingival inflammation is an individual trait (18). Trombelli et al. (19) previously showed that individual responses to induced gingivitis could be grouped into high and low clinical phenotypes, with the high response phenotype being linked to a persistent hyperresponsive parainflammatory state. Although nearly every human gingivitis study since 1965 (14, 17) has recognized there is variation in clinical parameters to bacterial dental plaque accumulation, resulting tin high and

Significance

Experimental gingivitis studies where dental hygiene is withheld from select teeth, allowing natural bacterial accumulation, provide a unique opportunity to study the reversible transition from health to inflammatory disease in humans. Longitudinal analysis of both the microbial and host changes during human experimental gingivitis revealed a previously unknown variation in the human host response and microbial succession sequence during inflammation. The significance of our findings can be summarized in two major points. First, the study comprehensively characterizes three different clinical responses—designated high, low, and slow—discerning unique host and microbial features that define each group. Second, we have unveiled previously unrecognized host protective mechanisms to prevent inflammatory bone resorption during reversible gingival inflammation.

Author contributions: S.B., G.A.K., J.S.M., and R.P.D. designed research; S.B., G.A.K., K.A.K., J.S.M., and R.P.D. performed research; K.A.K., J.S.M., and R.P.D. contributed new reagents/analytic tools; S.B., G.A.K., K.A.K., B.G.L., J.S.M., and R.P.D. analyzed data; and S.B., G.A.K., K.A.K., B.G.L., C.Z., D.C., H.M.T., J.S.M., and R.P.D. wrote the paper.

Competing interest statement: This work was funded in part by a Colgate-Palmolive clinical research grant (R.P.D., PI). This funding source had no role in the design of this study and did not have any role during its implementation, analyses, interpretation of the data, or decision to submit results.

This article is a PNAS Direct Submission.

[1]To whom correspondence may be addressed. Email: jsmclean@uw.edu or rdarveau@u.washington.edu.

This article contains supporting information online at https://www.pnas.org/lookup/suppl/doi:10.1073/pnas.2012578118/-/DCSupplemental.

Published June 30, 2021.

low clinical response phenotypes, the factors responsible for the significantly different individual host responses have not been elucidated. In this report, three different clinical response groups were identified and a granular parallel analysis of these groups revealed unique host and microbiome characteristics during induced inflammation.

Results

Variation in the Clinical Response to Human Experimental Gingivitis. In order to more fully explore the variation in the human host response to experimental gingivitis, we employed an experimental design that incorporated both early and late clinical evaluation and sampling time points (Fig. 1*A*). Clinical evaluation employed the standard measures of gingivitis, which are the gingival index (GI) (20) and bleeding on probing (BOP), both measures of gingival inflammation. Plaque index (PI) (21) was used to qualitatively measure visible bacterial accumulation on the tooth surface. As observed in numerous previous analyses (22), our study revealed dental plaque accumulation and clinical gingival inflammation in all study subjects (Fig. 2 *A–D*). In order to further understand the variability in the gingival host response, participants were clustered based on the joint clinical data trajectories of gingivitis severity represented by GI and BOP in response to plaque accumulation represented by PI on their test sides between day 0 and day 21. The clustering analysis was performed on all three parameters using the *k*-means for longitudinal data method in the "kml3d" R package (23) (*SI Appendix*, Fig. S1). This analysis revealed three distinct clinical response groups that were then designated as either high, low, or slow and represented 28.6%, 28.6%, and 42.9%, respectively, of the study participants (Fig. 1*B* and *SI Appendix*, Fig. S1). The high responder group included at a total of six participants (three male, three female, mean age: 20.67 ± 0.82 y), the low responder group also included a total of six participants (four male, two female, mean age: 24.5 ± 5.47 y), and the slow responder group included nine participants (four male, five female, mean age 24.33 ± 4.61 y). There were no statistical significant differences between the three groups in age [$F(2, 18) = 1.668$, $P = 0.216$] or sex ($\chi^2 = 0.73182$, $P = 0.6936$) (*SI Appendix*, Fig. S1).

However, in contrast, statistically significant differences in the trajectories of clinical parameters (PI, GI, BOP) from both baseline (day 0) and between the groups were evident (Fig. 2 *E–G* and *SI Appendix*, Table S1). As previously found, significant variations in the clinical response to gingivitis revealed both high and low clinical response groups (Fig. 2 *E–I*), with the low response group modulating GI and BOP between days 7 and 14, resulting in lower measures of inflammation (19). However, the inclusion of multiple early and late clinical evaluation measurements facilitated the identification of a novel slow host response group. These participants were characterized by a delayed increase in PI, which is visible microbial plaque accumulation and subgingival bacterial cell numbers as determined by quantification of 16S rRNA gene copies with a corresponding delay in clinical inflammatory indices (Fig. 2 *E* and *I*).

With the exception of significant differences at day 4 between the high and slow groups, with respect to gingival crevicular fluid (GCF) volume, there was no other significant difference between groups with respect to GCF volume (Fig. 2*H*) or neutrophil migration into the gingival crevice, as determined by quantitative ELISA determination of GCF myeloperoxidase (MPO) concentrations (Fig. 2*J*). In contrast to the similar neutrophil migration responses observed in the three groups, only the high response group displayed a significant increase in interleukin (IL)-1β levels at the end of the induction period (day 21), where clinical inflammation was the greatest (Fig. 2 *K* and *L*). Notably, at peak inflammation at day 21, IL-1β levels within the high group are significantly different ($P < 0.05$) than the slow group subjects, which are tightly clustered around the time of inclusion (day −14) and control side levels despite displaying similar clinical inflammation (GI and BOP) as the high responder group by day 21 (Fig. 2 *K* and *L* and *SI Appendix*, Table S2). Within-group variability was relatively equal for the clinical and above-mentioned

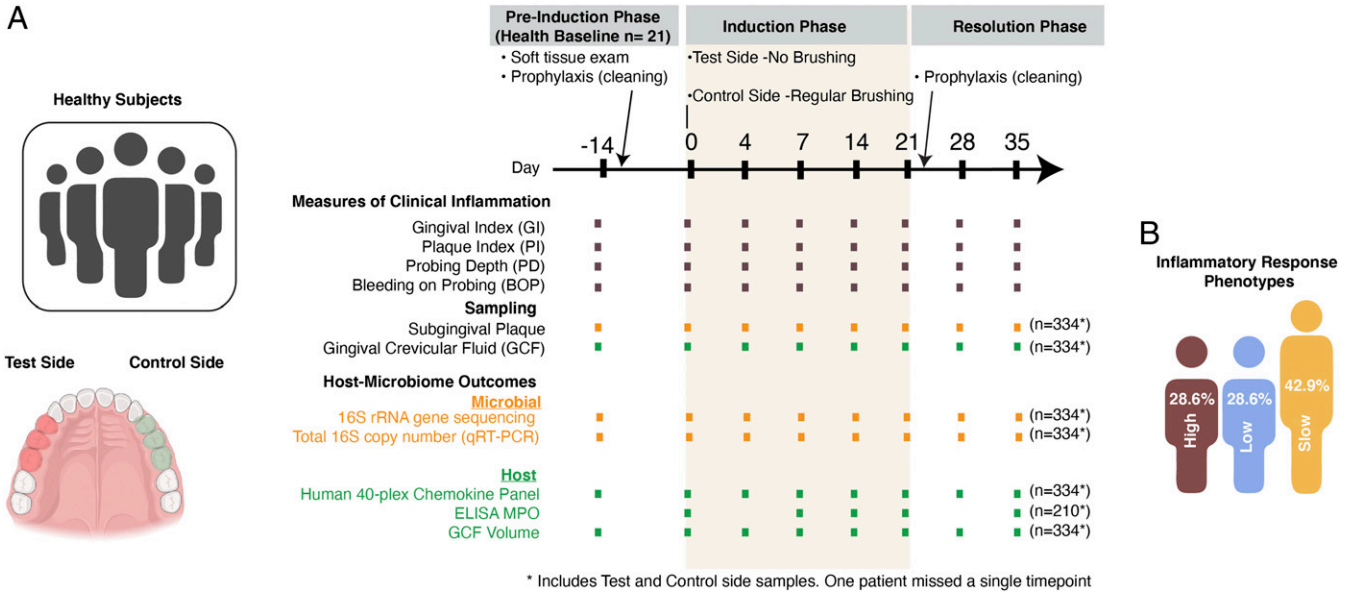

Fig. 1. Experimental gingivitis study design. (*A*) Experimental cessation of oral hygiene leads to increased plaque biomass and induced gingivitis. Within-subject contralateral teeth with regular oral hygiene served as controls. Baseline was established from day −14 to day 0. Induction of experimental gingival inflammation was carried out from day 0 through day 21. Resolution of experimental gingivitis was observed from day 21 until day 35 when no residual clinical inflammatory activity was detectable (see *SI Appendix, Supplemental Materials and Methods*). Comprehensive clinical, chemokine and microbiome analysis were conducted to obtain highly granular multiplexed analyses of changes during induction and resolution of inflammation. (*B*) Percentages of subjects that were clustered into the three clinical response groups (high, low, and slow) based on longitudinal trajectories of clinical parameters (GI, PI, and BOP) (*SI Appendix*, Fig. S1).

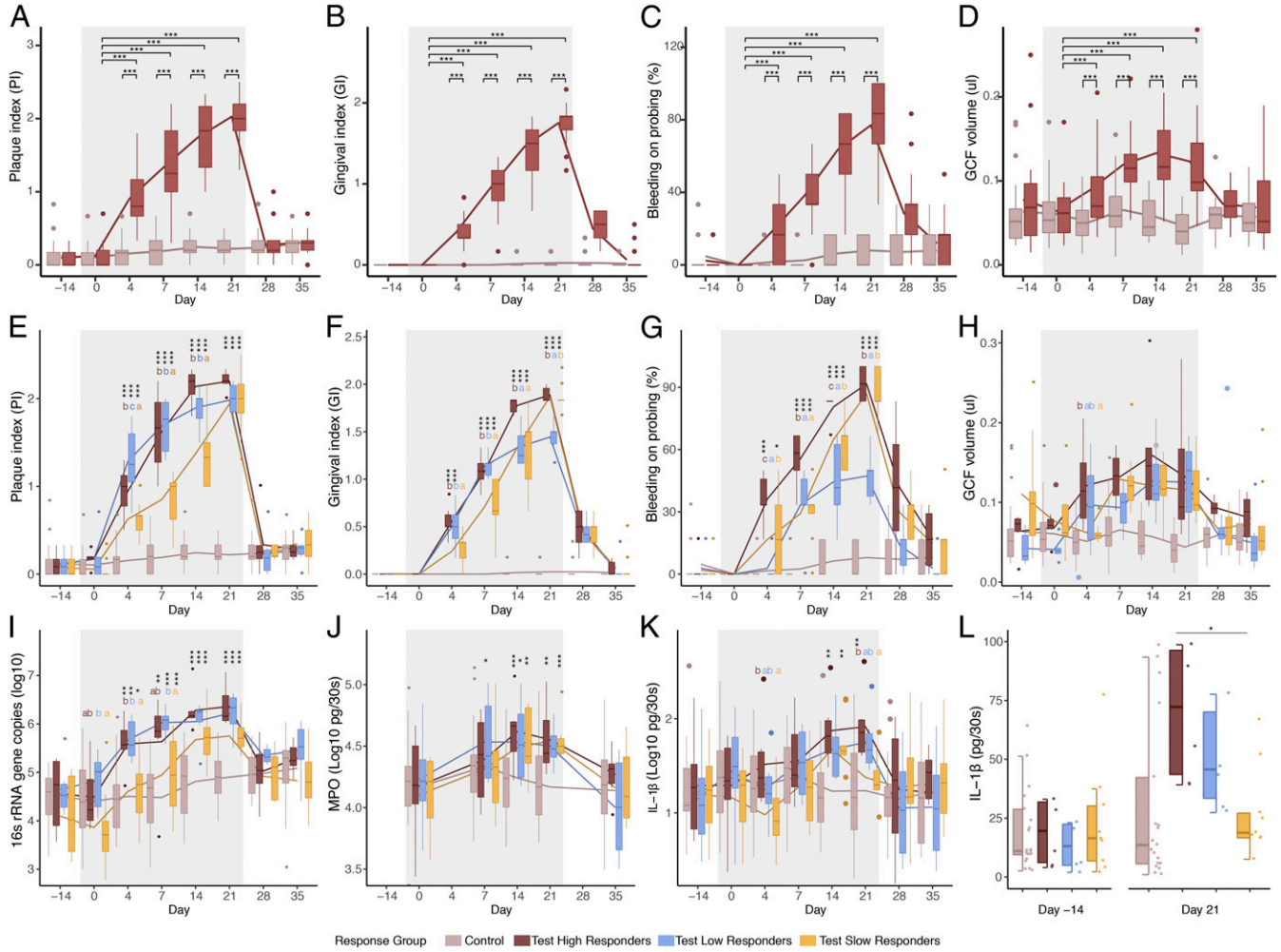

Fig. 2. Differential clinical inflammatory responses and chemokine levels in the three response groups versus controls. (*A–D*) Distributions of clinical parameters comparing test side (no-brushing) versus control side (brushed) for all subjects over time. (*E–H*) Temporal changes in inflammatory-associated clinical measures stratified by response group (high [n = 6], low [n = 6], slow [n = 9]). (*I–L*) Responses among sample-sites in each of three clinical inflammatory response groups (high, low, and slow) before, during, and after resolution of bacterial-induced inflammation. (*I*) Bacterial load based on total 16S rRNA gene copies; y axis $\log_{10}$-scaled. (*J*) Neutrophil marker MPO. (*K* and *L*) proinflammatory cytokine IL-1β. Boxes represent data and medians ± interquartile ranges (IQR); whiskers and outliers > 1.5 IQR below (above) the 25th (75th) percentile. Trend lines represent mean values across time points. Different letters above bars indicate the significant differences between groups at that time point (a, b, c) (FDR $P < 0.05$). In *A–D* statistical analyses were performed against the controls by comparing all test samples (prior to responder group identification) and all pooled data from the control teeth data (intraoral control) for just these select clinical parameters and only calculated for the induction phase. In *E–L* the responder groups are shown in relation to the pooled control group. Control samples were never physically pooled; however, the data, for clarity in the figures, was reduced from the total six groups (three test and three control) to four groups (three test and one pooled control). Differences of each group compared to baseline (day 0) are shown above the groups and their significance level indicated by asterisks. Significance levels: *$P < 0.05$, **$P \leq 0.01$, and ***$P \leq 0.001$. (*L*) Comparison of IL-1β levels between groups at peak clinical inflammatory endpoint (day 21) show the subjects in the slow group were significantly different from the high responder group that displayed elevated IL-1β.

parameters, with no response group displaying a consistently higher or lower variability over the study period.

Chemokine Utilization Is Significantly Altered during Experimental Gingivitis. Differences in the host inflammatory mediator response between the three different clinical responder groups was performed with a bead-based multiplex analysis (Bio-Plex Pro Human 40-plex Chemokine Panel). Fig. 3*A* displays the normalized (row-wise z-score) log mean values for the expressed chemokines (picograms per 30-s sample) in each responder group, as well as the contralateral control teeth (all responder groups combined for control teeth) at the indicated day. Comprehensive analysis of host inflammatory mediators elicited by the different clinical responder groups revealed significant changes in overall chemokine expression patterns. Most notably, it was found that the low clinical responder group displayed several SDs below the mean of all the groups in most chemokines. This is consistent with these individuals demonstrating the lowest levels of clinical inflammation throughout this experimental gingivitis study (Fig. 2 *E–G*).

Upon more detailed examination, the levels of the major neutrophil chemokines observed on the panel revealed nearly all neutrophil chemokines examined in this study either decreased or did not significantly increase during experimental gingivitis (Fig. 3 and *SI Appendix*, Fig. S2 and Table S2). Of particular note is the observation that IL-8/CXCL8 and GCP-2/CXCL6 (Fig. 3 *C–H*), two chemotactic and neutrophil-activating chemokines, did not increase during experimental gingivitis, which is consistent with the reported difference in the neutrophil phenotypes found in gingivitis (24). In contrast to the decreases found in neutrophil chemokine expression, macrophage inhibitory factor (MIF), which has been reported to

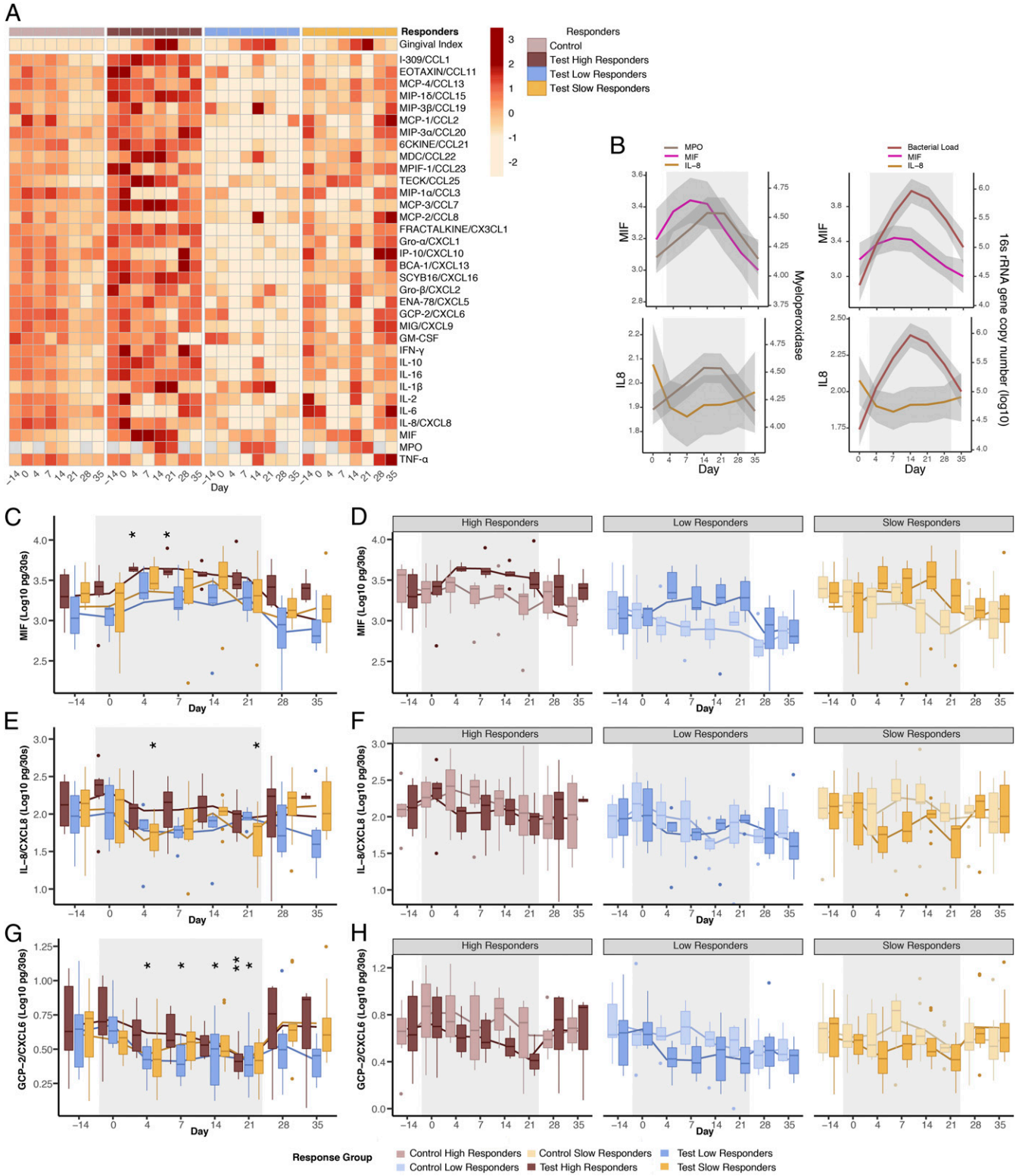

Fig. 3. Relationship between chemokine levels and the three clinical response groups. (*A*) Normalized (row-wise *z*-score) mean values for chemokine expression by responder groups and controls (all responder groups' control side data are combined for clarity) by day. The low responder group displays several SDs below the mean of all the groups in most chemokines. (*B*) Temporal relationships between major neutrophil chemokines IL-8/CXCL8 and MIF with MPO and bacterial load. MIF demonstrated an inverted U-shape distribution during the induction-resolution human experiment that was similar to the temporal changes in microbial load (negative quadratic coefficients; $P < 0.01$ for both MIF and bacterial load). MPO changes followed the same temporal pattern as MIF (negative quadratic coefficient; $P < 0.001$), while IL-8/CXCL8 levels demonstrated a U-shape distribution with no association to MPO levels (positive quadratic coefficient; $P = 0.09$). (*C*–*H*) Temporal changes in major neutrophil chemokines (MIF, IL-8/CXCL8, and GCP-2/CXCL6) across responder groups compared to each of the responder groups (*C*, *E*, *G*) and between their respective control side sample in the split-mouth design (*D*, *F*, *H*). Boxes represents data and medians ± IQR; whiskers and outliers > 1.5 IQR below (above) the 25th (75th) percentile. Trend lines represent mean values across time points. For *D*, *F*, and *H*, separate controls for each group in were displayed against their respective healthy controls. Differences of each group compared to baseline (day 0) are shown above the groups and their significance level indicated by asterisks. Significance levels: $*P < 0.05$ and $**P \leq 0.01$.

demonstrate neutrophil chemotactic activity (25), trended toward increased expression in all clinical response groups and was significantly increased compared to baseline values (day 0) in the high response group on days 4 and 7 (Fig. 3 *C* and *D*). In fact, granular analysis of early gingival inflammation (days 0 to 4) groups revealed that neutrophil migration into the gingival sulcus changed in response to MIF and not IL-8/CXCL8 levels over time (Fig. 3*B*). Since the experimental induction and resolution interventions led to an inverted U-shape and the increase in MIF and neutrophil migration ($P < 0.0001$), as well as the decrease in IL-8/CXCL-8 ($P < 0.0001$), occurred in all clinical response groups (Figs. 2 and 3), the analysis was performed with quadratic regression models combining all the clinical response groups. The time-course distributions of MIF and MPO mirrored one another, with changes in MIF level preceding concordant MPO levels (Fig. 3*B*). The temporal changes in bacterial load, MPO, and MIF had very similar patterns across induction and resolution time points, while IL-8/CXCL-8 levels did not significantly change ($P = 0.09$) (*SI Appendix*, Fig. S3).

Bone and Tissue Chemokine Modulators Are Significantly Altered during Experimental Gingivitis. We further investigated the lack of a strong host chemokine response among individuals within the low inflammatory response group (Fig. 4). This analysis revealed that MIP-1α/CCL3, a homeostatic regulator of bone resorption (26, 27) and a proposed biomarker of periodontitis (28), was significantly reduced in all three clinical response groups at the first gingivitis measurement (day 4) and was restored at the first time point in the resolution phase (day 28) (Fig. 4*A*). Furthermore, it was found that five additional chemokines (MCP-1/CCL2, MIP-3α/CCL20, SCYB16/CXCL16, GRO-α/CXCL1, and MPIF-1/CCL23), which have been shown to contribute to either normal bone turnover processes or inflammatory bone loss during periodontitis (29–35), displayed overall significantly lower chemokine levels within the low response group when compared to the high response group (Fig. 4 *B*–*F* and *SI Appendix*, Table S2).

Characterization of the Microbial Compositional Changes in the Different Clinical Response Groups. The high-resolution DADA2 approach for 16S rRNA gene data implemented in QIIME2 (36) was used to determine the unique amplicon sequence variants (ASVs) for the dataset ($n = 11{,}885$ in 334 samples). Changes in the α-diversity within the microbial community for all subjects' test and control sides (*SI Appendix*, Table S3), as well within each clinical response group (*SI Appendix*, Table S4) during gingivitis induction, was examined using five different metrics across different time points. At the time of inclusion and baseline (day −14 and day 0), there were no significant differences in any of α-diversity or β-diversity indices between control and test sides or between the response groups (Fig. 5 *A* and *B*). This lack of diversity and compositional differences between groups, prior to and after the first cleaning, was not unexpected given that these were all relatively young and healthy subjects with regards to oral health. In general, all α-diversity metrics using ASV data showed an increase above the control side during the induction phase (day 0 to day 21), corresponding to increased gingivitis severity (Fig. 5*A* and *SI Appendix*, Table S4).

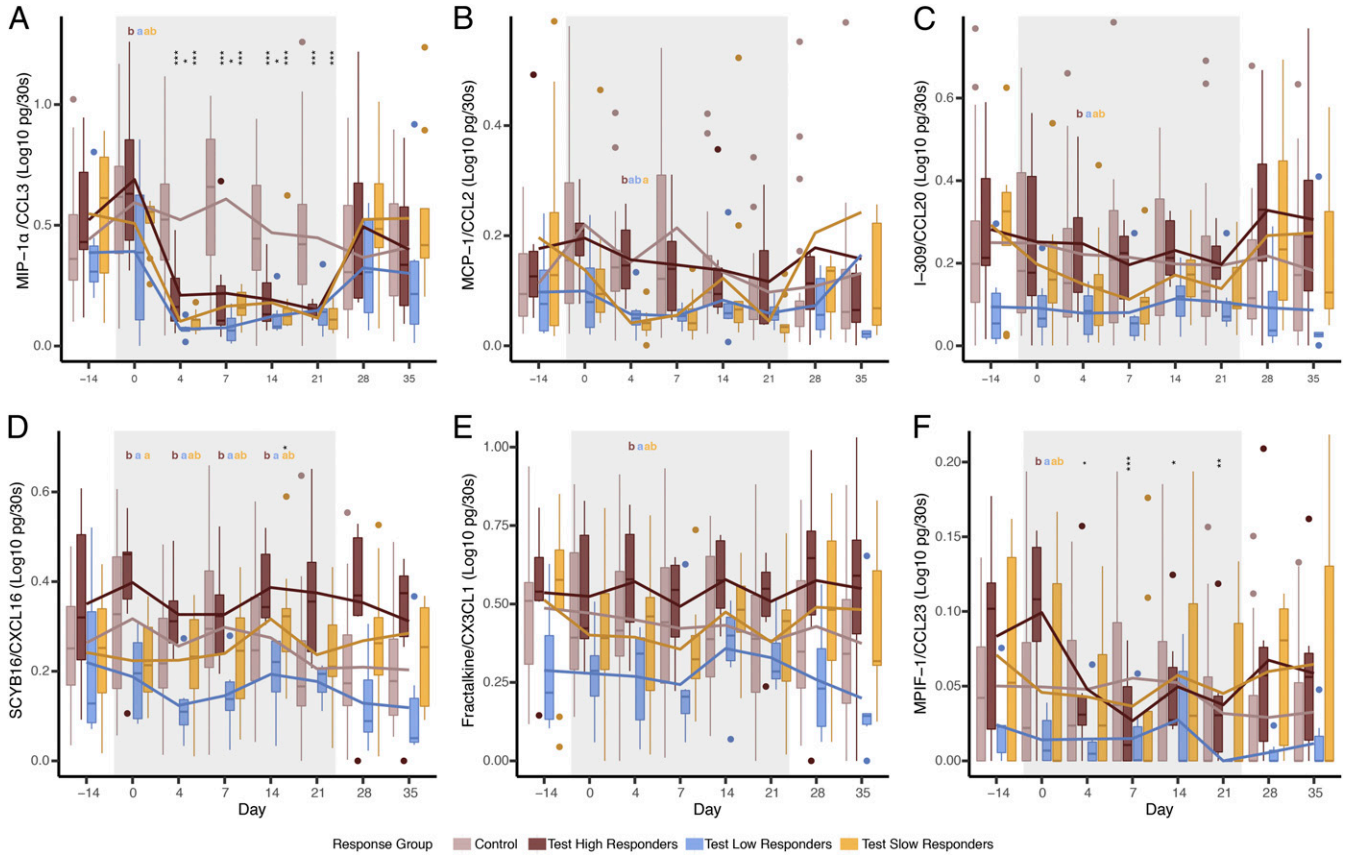

Fig. 4. (*A*–*F*) Changes in levels of chemokines involved in bone homeostasis following induction of reversible bone-sparing gingival inflammation. Responses among sample-sites in each of three clinical inflammatory response groups before, during, and after resolution of bacterial-induced inflammation. Boxes represents data and medians ± IQR; whiskers and outliers > 1.5 IQR. Trend lines represent mean values across time points. Different letters above bars indicate the significant differences between groups at that time point (a, b, c) (FDR $P < 0.05$). Differences of each group compared to baseline (day 0) are shown above the groups and their significance level indicated by asterisks. Significance levels: $*P < 0.05$, $**P \leq 0.01$, and $***P \leq 0.001$.

β-Diversity analysis revealed shifts in community composition over the same period (Fig. 5*B*). Together, both α- and β-diversity showed a return to highly similar compositions after resolution (days 28 and 35). Notably, as early as day 4, the slow response group demonstrated a distinct delay in phylogenetic diversity (Fig. 5*A*) and showed a trend toward separation in β-diversity from the high and low response groups, which remained more similar to the control side (Fig. 5*B*). This observation was consistent with the rapid accumulation of plaque and development of inflammation in high and low compared to slow responders (Fig. 2 *E*–*G* and *I*).

Taxonomic analysis of subgingival plaque samples during the onset of experimental gingivitis confirmed the well-known and characteristic shift (37, 38) from a health-associated gram-positive to a disease-associated gram-negative composition associated with gingivitis. For example, in all three clinical response groups, the two most-abundant gram-positive phyla, Firmicutes and Actinobacteria, decreased in relative abundance (Fig. 5*C*). In contrast, the most-abundant gram-negative phyla, Bacteroidetes, increased in its relative abundance (Fig. 5*C*). However, group-level analysis at the genus level revealed novel differences in the relative abundance profiles during the development of gingivitis among the three different response groups (Fig. 5 *D*–*F* and *SI Appendix*, Fig. S4 and Table S5). An increase in genera within the phylum Bacteroidetes was not uniform across all three clinical response groups described in this study. For example, *Tannerella* increased late in gingivitis in both low and slow response groups, but was dramatically reduced in comparison to the high response group (Fig. 5*E*). In contrast, *Prevotella* displayed the greatest increase within the low response group, even though the high and slow groups eventually showed a significant increase later during gingivitis development (Fig. 5*E*). Other abundant gram-negative–associated genera, such as *Porphyromonas* and *Fusobacterium*, also displayed intergroup variations

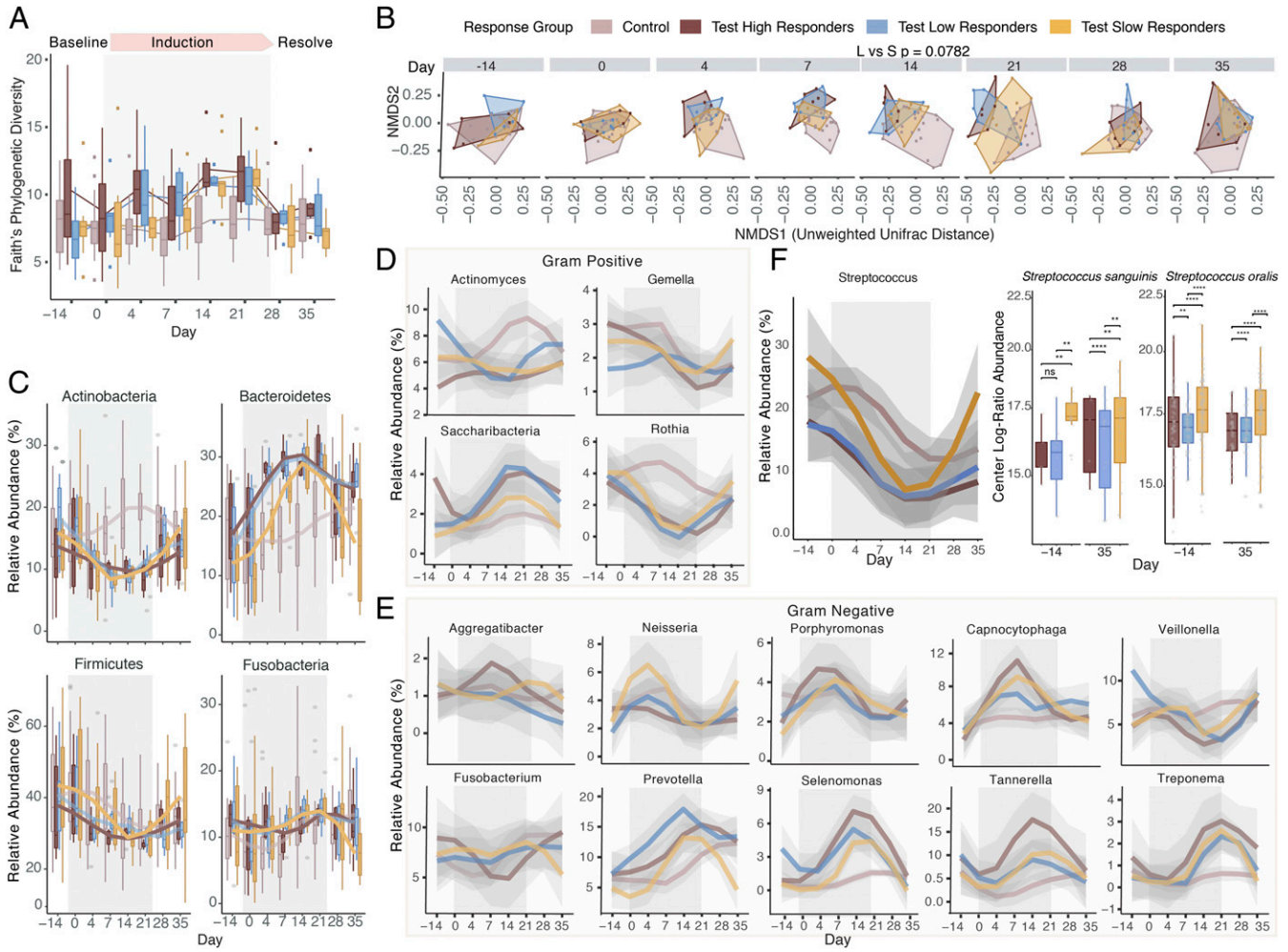

Fig. 5. Temporal changes in microbial diversity and taxonomy vary by inflammatory responder type. (*A*) Faith's phylogenetic diversity by responder group and controls from day −14 to day 35 (n = 334 samples from 21 subjects). Boxplots show median and 25th/75th quartiles; whiskers show inner fences. Lines show mean richness by clinical responder group (high, low, and slow) and controls (within-subject noninflamed gingival sites). (*B*) Nonmetric multidimensional scaling (NMDS) plots of β-diversity (unweighted Unifrac distance matrices) by responder group and controls from day −14 to day 35 (n = 334 samples from 21 subjects). Tests for significance in β-diversity between groups determined by PERMANOVA. (*C*) Phylum-level distributions of relative abundance by responder group and controls from day −14 to day 35 (n = 334 samples from 21 subjects). (*D* and *E*) Genus-level mean relative abundance by responder group and controls from day −14 to day 35. Linear regression (Loess) shown with 95% confidence bound (*SI Appendix, Supplemental Materials and Methods*) (n = 334 samples from 21 subjects). (*F*) *Streptococcus* mean relative abundance by responder group and controls from day −14 to day 35 (n = 334 samples from 21 subjects). Also shown are center log-transformed (CLR) relative abundances of ASVs taxonomically assigned to *S. sanguinis* and *S. oralis* species in high, slow, and low inflammatory response groups from day −14 and day 35. Boxplots show median and lower/upper quartiles; whiskers show inner fences (*Materials and Methods*) (n = 84 from 21 subjects), (Wilcoxon test; adjusted by FDR) (*SI Appendix, Supplemental Materials and Methods* and Table S5). Asterisks show FDR-corrected statistical significance levels (FDR $^{**}P \leq 0.01$ and $^{****}P \leq 0.0001$).

throughout the induction phase (day 0 to day 21). Interestingly, a gram-positive member of the candidate phyla radiation, "*Candidatus* Saccharibacteria" (formerly TM7), which are ultrasmall parasitic bacterial epibionts (39), selectively increased during the induction phase among high and low responders, but not in the slow response group.

Consistent with the changes in α- and β-diversity, the most notable differences overall were observed in the slow response group, with the rate of Firmicutes decreasing and the concomitant increase in Bacteriodetes being markedly delayed (Fig. 5*C*). At the genus level, *Streptococcus*, which is a member of the phyla Firmicutes, decreased at a slower rate in comparison to the high and low groups, and was initially higher at the time of inclusion and baseline (day −14 and day 0), and even regained prominence at the end of the study (day 35) (Fig. 5*F*). The observed delay in both the α- and β-diversity among the slow response group is, therefore, most likely a consequence of the prolonged presence of *Streptococcus*, which is both the most abundant genera within the healthy subgingival pocket and uniquely characteristic of this response group. These observations are entirely consistent with the distinct delay in the clinical manifestations of gingivitis within the slow group (Fig. 2 *E*–*G*). Of particular note, we observed that the slow group had statistically significant higher relative abundance of ASVs classified as *Streptococcus sanguinis* and *Streptococcus oralis* species at the time of inclusion and at baseline (day −14 and day 0), as well as during resolution phase at the end of this study (day 35), which resulted in trends toward preinduction levels (Fig. 5*F*).

Overall, the trajectory of the slow response group can be readily discerned from the other community profiles and, as shown above, this group can elicit significantly lower IL-1β responses (Fig. 2 *K* and *L*). In contrast, the high and low clinical response groups displayed a lack of clear separation in α- and β-diversity measures during the microbially induced inflammation, which correlates with their highly similar plaque accumulation rates (Fig. 2*E*).

Discussion

The human experimental gingivitis model provides a unique opportunity to study bacterial community succession during plaque accumulation and the subsequent host response in real time (14). The first human experimental gingivitis study (14), as well as several subsequent studies (17–19), have identified high and low clinical response groups based upon the GI, a measure of local gingival inflammation. In our study, these two clinical host response groups were also found and were characterized by significantly lower GI and BOP within the low response group compared to the high response group (Fig. 2 *F* and *G*). Furthermore, by conducting a longitudinal trajectory-based clustering of inflammatory changes, compared to cross-sectional clustering previously performed, an additional slow clinical response group characterized by a delayed increase in microbial plaque accumulation and a corresponding delay in clinical inflammatory indices was identified (Fig. 2 *E*–*G*).

Characterization of the clinical response groups revealed previously unrecognized variability in the microbial succession and host response that occurs during gingivitis. Here we observed that the α-diversity within the slow response group showed a completely separate community in terms of both the rate of plaque growth and community compositional changes in comparison to the high and low response groups (Figs. 2*E* and 5*A*), together demonstrating the great degree of variation in gingivitis within the human population. Variation in plaque accumulation rates in the human population have been reported previously (40); however, this has not been reported in association with subgingival plaque rates or in regards to the impact on inflammation. In this study, which defines three clinical response groups, we found the slow response group had statistically significant higher relative abundance of ASVs classified as *S. sanguinis* and *S. oralis* species at day −14, at the time of inclusion prior to the start of the study, and day 35 during the resolution phase (Fig. 5*F*). This suggests the possibility that participants belonging to the slow response group may be identifiable prior to the study and are predisposed to reduced plaque formation rates and a slower shift to gram-negative species. This delay in the gram-negative shift, where inflammophilic bacterial (41) species increase in relative abundance, may contribute to less-frequent episodes of gingivitis in these individuals. The genus *Streptococcus* is composed of predominantly health-associated species known to inhibit other gram-negative species by the production of bacteriocins and hydrogen peroxide. *S. sanguinis* and *S. oralis* species have been shown to inhibit *Aggregatibacter actinomycetemcomitans*, *Porphyromonas gingivalis*, and *Prevotella intermedia* (42); therefore, by remaining persistent within the community at a high abundance, they may be delaying the overall microbial succession and plaque growth rates seen in the high and low response groups during the onset of experimental gingivitis.

It was also observed that the lack of expression of IL-1β in the slow clinical response group did not significantly contribute to gingival inflammation among individuals within this group, even though this inflammatory mediator has been considered a hallmark of gingival inflammation and repeatedly shown to be strongly associated with experimental gingivitis in a number of clinical studies (43–47). Therefore, the significantly different IL-1β responses in the high and slow clinical response groups clearly demonstrates that multiple inflammatory etiologies can elicit the clinical manifestations of gingivitis. It is not known at this time if a different microbial composition or a unique inflammatory phenotype accounts for the lack of IL-1β expression in these individuals. However, the data underscore the need for further characterization of the different gingivitis phenotypes to administer effective therapeutic interventions.

In contrast to the slow clinical response group, both the high and low clinical response groups displayed a similar rapid increase in bacterial plaque accumulation and microbial ecological succession patterns. Although several differences in the microbial composition were noted, the overall lack of host chemokine inflammatory mediator expression with a high microbial load is strongly suggestive that in low clinical response individuals it is the host response, as opposed to the microbial composition, that is primarily responsible for the low gingival inflammation. This was observed in that both the GI and most notably the BOP scores never attained the same degree of clinical inflammation in comparison to the high clinical response group, although the microbial load continued to increase until the end of the induction phase of the study (day 21). Furthermore, it was found that five chemokines (MCP-1/CCL2, MIP- 3α/CCL20, SCYB16/CXCL16, GRO-α/CXCL1, and MPIF-1/CCL23), which have been shown to contribute to either normal bone turnover processes or alveolar bone loss during periodontitis (31–33, 35, 48), displayed overall significantly lower chemokine levels in our low response group when compared to our high response group (Fig. 4). However, further investigations are needed to determine if minor microbiome differences or host immune variability, or both, contribute to the difference between high and low clinical response groups.

Examination of chemokines that regulate neutrophil migration revealed that all individuals, regardless of their clinical response phenotype, modulated expression of neutrophil activation. Healthy gingival homeostasis requires a chemokine-controlled neutrophil migration process from the gingival vasculature, through the junctional epithelium, and into the gingival crevice (6). In mice, this process has been shown to require select chemokine receptors (9, 10) and ligands, as well commensal bacterial colonization (12, 49). In humans, IL-8/CXCL8 has been shown to be selectively expressed in clinically healthy junctional epithelial tissue, providing a concentration gradient for constant neutrophil surveillance of the periodontium (6). However, during experimental gingivitis it was found that this process was disrupted in that the levels of five (IL-8/CXCL8, GRO-α/CXCL1, GRO-β/CXCL2, ENA-78/CXCL5, GCP-2/CXCL6) of the six neutrophil chemokines we examined did not

increase, even though more neutrophils migrated into the junctional epithelium and is typically observed in gingivitis (50).

Although a decrease in IL-8/CXCL8 during gingivitis has been previously reported by several groups (44, 47, 51), the more extensive failure to increase a variety of other neutrophil chemokines has not been previously reported. In contrast, MIF, not previously recognized as a major gingival-associated neutrophil chemokine although reported to be present in GCF (52), increased in all response groups after the induction of experimental gingivitis. In fact, analysis comparing MIF, IL-8/CXCL8, and neutrophil migration clearly demonstrated that MIF replaced IL-8/CXCL8 as the neutrophil chemokine that recruits neutrophils during experimental gingivitis (Fig. 3*B*). The decrease in two CXCR1 neutrophil-activating chemokines, GCP-2/CXCL6 and IL-8/CXCL8, provides a mechanism for the reduced neutrophil activation state previously described during experimental gingivitis (24). In addition, the selective increase in MIF, which does not engage the neutrophil-activating receptor CXCR1 (53), provides a mechanism by which neutrophil migration is maintained without activation and potential tissue damage during experimental gingivitis in each clinical response group. However, due to the association between MIF and alveolar bone loss, it is possible that continued MIF secretion may directly or indirectly contribute to bone loss in the transition from gingivitis to periodontitis (54).

Experimental gingivitis also modulated the expression of MIP-1α/CCL3, a bone remodeling chemokine through activation of osteoclastogenesis (29). Furthermore, because it is well established that the parainflammatory state during episodes of gingivitis can develop into periodontitis (22), significantly lower levels of MIP-1α/CCL3 in all response groups may represent a previously unrecognized host protection mechanism to protect against bone loss during gingivitis. Consistent with this, it has been previously demonstrated that germ-free mice display an increase in alveolar bone height, revealing the contribution of oral commensal bacteria to oral alveolar bone homeostasis though a balance of osteoblastogeneisis and osteoclastogenesis (11, 12). Significant reduction in MIP-1α/CCL3 in all clinical response groups is consistent with a change in alveolar bone homeostasis that favors less bone resorption. The shift in both neutrophil activation and bone homeostasis mediators reveals a previously unrecognized host response mechanism that serves to protect the host from localized tissue and bone damage during periods of gingival inflammation.

This study has several strengths, including the incorporation of a large panel of subgingival GCF mediators and culture-independent subgingival plaque microbiomes in parallel at high temporal resolution, including capturing changes as early as day 4. The present study also has some limitations. Results should be interpreted with caution due to the small sample size. Although the number of subjects was just 21, there were 42 samples at each time point (including test and control sides) for a total of 336 samples (210 total samples for the induction-phase experimental time points) for each measured parameter. However, with the sample size being 42 (including test and control sides) and the number of independent observations being 21, statistical power for some analyses was limited. In addition, as is typical with the analysis of high-dimensional datasets as with this study, a large number of statistical tests were performed, which raises the likelihood of some false-positive results. Hence, the results should be viewed as hypothesis-generating and replication of the results is needed. However, it also should be noted that several of the findings reached a very high level of statistical significance ($P < 0.001$), which lessens concerns about limited power and false positives.

In conclusion, by providing the most comprehensive temporal characterization of human inflammatory responses to oral bacterial-induced inflammation, we identified three distinct clinical phenotypes inducing a high, low, or slow gingival inflammatory response. The slow clinical inflammatory phenotype was characterized by linear responses to microbial biomass accumulation in the gingiva and exhibited higher relative abundances of *Streptococcus* spp. than the other phenotypes, which led to a clinically more resistant homeostatic state. In addition, it is particularly noteworthy that the slow clinical response group did not contain high gingival crevicular fluid levels of IL-1β, revealing a novel inflammation response for this group of individuals. In contrast, the high and low clinical response groups demonstrated strikingly similar microbial succession patterns that led to significantly different inflammatory responses.

Furthermore, two protective mechanisms were identified. First, although during bone destructive periodontitis neutrophil migration is associated with an increase in IL-8/CXCL8 in the junctional epithelium (6), in reversible bone sparing gingival inflammation, MIF, a neutrophil chemokine not normally associated with healthy homeostasis increases, demonstrating a shift in the neutrophil recruitment regime during gingivitis. Importantly, MIF-mediated neutrophil recruitment is associated with an alternative neutrophil chemokine expression regime with near shut down of CXCR1-binding chemokines GCP-2/CXCL6 and IL-8/CXCL8, which activate the oxidative killing pathway that causes tissue collateral damage (24, 55). The lack of activation of neutrophil oxidative killing during gingivitis has been reported previously as a tissue saving response (24); however, the mechanism for this has not been previously shown. Second, MIP-1α/CCL3, a chemokine associated with bone homeostasis (26), is completely shut down during experimental gingivitis, indicative of a significant alteration in bone turnover processes. Collectively, these findings pave the way for the more attention to be paid to individual differences in both the microbial composition and host response to more fully understand bacterial dysbiosis-driven diseases.

Materials and Methods

Human Induced Gingivitis Experiment. The study methodology was based on the established protocol by Löe et al. (14) for induction of reversible bacterial-induced inflammation via cessation of oral hygiene in humans. Our full study protocol was approved by the University of Washington's Institutional Review Board (HSD# 50151). Twenty-one generally healthy adults aged 18 to 35 y gave consented and enrolled. For inclusion, subjects had gingival health with no clinical signs of gingival inflammation at >90% of sites at time of screening and had no signs of periodontal disease. Detailed inclusion and exclusion criteria are presented in *SI Appendix, Supplementary Materials and Methods*. The study included the following phases: 1) preinduction phase with normal hygiene for 2 wk prior to baseline (day −14 to day 0); 2) gingivitis induction phase lasting for 3 wk (day 0 to day 21); and 3) resolution phase for 2 wk (day 21 to day 35) (Fig. 1). During the experimental induction phase, the subjects were given customized intraoral stents with detailed instructions for use during regular brushing, with the purpose of preventing accidental brushing of the experimental sites. Fidelity monitoring of the intervention was conducted at each time point throughout the experiment by clinical assessment of the plaque index. The different clinical response groups were identified at the end of the study, as described in *SI Appendix*, Fig. S1.

Characterization of In Vivo Chemokine Responses during Experimental Gingivitis. At each time point, local chemokine responsiveness was measured in gingival transudate (i.e., GCF). Eight index tooth sites were isolated and sampled without disrupting supragingival plaque by gentle insertion of sterile paper strips (Periopaper; Oraflow Inc.) into the gingival crevice. Samples from the sites were pooled and placed immediately on ice and transported to the laboratory for processing. Samples from contralateral control teeth were also collected. The volume of GCF samples was collected and immediately quantified with a previously calibrated measuring device (Periotron 8010; OraFlow Inc.). GCF samples were eluted to retrieve GCF proteins as described in *SI Appendix, Supplementary Materials and Methods*. The concentrations of MPO, a good marker of neutrophils infiltration (56), were quantified using a commercially available ELISA kit and simultaneous quantification of multiple chemokines was performed via a 40-plex chemokine bead-based multiplex assay (Bio-Plex Pro Human 40-plex Chemokine Panel; Bio-Rad Laboratories).

Characterization of Microbial Changes in Response to Plaque Accumulation. Subgingival plaque samples were collected at each study visit from both control and test sides. Sterile paper points were inserted into the gingival

sulcus of the six maxillary teeth for 30 s. At each study visit, a total of six samples per study side were collected and pooled and samples were transported to the laboratory on ice and then frozen at −80 °C until further analysis. DNA was extracted and 16S rRNA libraries were created as previously described (57, 58). For DNA extraction negative controls were implemented by performing the DNA extraction protocol without plaque samples with either kit reagents only or kit reagents with the sterile paper points to assess for contamination. In addition, to validate the efficiency of the technique, positive controls using known bacterial cultures were included. Quantitative real-time PCR was performed to determine the total bacterial load in each sequenced sample. A qPCR standard curve was generated from serially diluted *Fusobacterium nucleatum* ATCC 10953 genomic DNA.

Analysis of merged 300-bp paired-end reads (average length 450 bp) was performed as previously described (57, 58) using the Quantitative Insights into Microbial Ecology (QIIME2, version 2018.2) (59) following the Divisive Amplicon Denoising Algorithm 2 (DADA2) pipeline workflow (36, 60) to generate ASVs. Taxonomic assignment to classify ASVs was performed using the Human Oral Microbiome Database (HOMD 16S rRNA RefSeq v15.1) (61, 62). Data were integrated into a single object using the "phyloseq" R package (63) and further analyzed (*SI Appendix, Supplementary Materials and Methods*).

Variation in Clinical Gingival Inflammatory Responses. Clinical data, including PI (21), GI (20), and BOP, were assessed at each time point as measures of clinical inflammation. All measurements were performed by a single, trained examiner using the same type of graded periodontal probes during the following study phases: preinduction phase (days −14 to 0), induction phase (days 4, 7, 14, and 21), and resolution phase (days 28 and 35) (Fig. 1*A*). To identify clusters of inflammatory responses among participants, we assessed joint clinical data trajectories of gingivitis severity represented by GI and BOP in response to plaque accumulation represented by PI from day 0 to day 21 in the test sides using an implementation of *k*-means specifically design to cluster joint trajectories (23, 64).

Statistical Analysis. Clinical and mediator data were summarized into single average scores for test and control per person at each time point and were reported using boxplots showing medians and interquartile ranges. The comparisons between test and control sides over time were performed using linear mixed-models with individual subjects as random effects and implemented in the "*lme4*" package version 1.1-27 (65) in R statistical software. Fixed-effects comparisons between test and control sides, and over-time changes within each group, were performed and post hoc false-discovery rate (FDR) (66) corrected pairwise comparisons were reported using the emmeans() function in the "*emmeans*" package in R (67). As summarized above, statistical tests based on a linear mixed-model were used to compare clinical and chemokine data between different responder groups during the induction phase (days 0, 4, 7, 14, and 21), and within each responder group between baseline (day 0) and different time points during the induction phase (day 4, 7, 14, and 21).

To determine the mechanisms responsible for homing neutrophils through inflamed oral junctional epithelia in bacterial-induced inflammation, we analyzed the distributions of neutrophil MPO levels, which are reflective of neutrophil numbers, and known mediator chemokines responsible for neutrophil migration over time. Because the experimental bacterial-driven induction and resolution of gingivitis led to an inverted U-shape distribution of bacterial biomass (total bacterial 16S rRNA gene copies) in vivo, we employed quadratic regression models to better study the temporal changes of MPO and the two major neutrophil signaling chemokines: MIF and IL-8/CXCL8 in response to microbial accumulation across study time points. Quadratic regression models were implemented in R using second degree polynomials and coefficient directions and *P* values representing the quadratic terms are reported.

Data Availability. Raw read and sample meta data have been deposited in the National Center for Biotechnology Information Sequence Read Archive, https://www.ncbi.nlm.nih.gov/sra (BioProject PRJNA615201) (68). The data that support the findings of this paper and the R code used for generating the analysis has been made publicly available in the format of an R markdown (PDF and .html) published on a GitHub repository (https://github.com/mcleanlab/HVGI_Study) (69). This HGVI repository contains all necessary raw and processed files, (i.e., .biom, metadata.txt, .tree) to recreate these analyses as well as additional supplemental material derived from this study.

ACKNOWLEDGMENTS. Statistical analyses were supported by the statistics core of the Translational Periodontal Research Laboratory, University of Texas Health San Antonio, funded in part by NIH DE029872 (to G.A.K.). The research was also funded in part by NIH TR002318, T90 DE021984 (to K.A.K.), and DE023810, DE027199 (to J.S.M.).

1. R. Medzhitov, Origin and physiological roles of inflammation. *Nature* **454**, 428–435 (2008).
2. M. Chen, H. Xu, Parainflammation, chronic inflammation, and age-related macular degeneration. *J. Leukoc. Biol.* **98**, 713–725 (2015).
3. N. Fine *et al*., Distinct oral neutrophil subsets define health and periodontal disease states. *J. Dent. Res.* **95**, 931–938 (2016).
4. L. V. Hooper, Bacterial contributions to mammalian gut development. *Trends Microbiol.* **12**, 129–134 (2004).
5. R. P. Darveau, Periodontitis: A polymicrobial disruption of host homeostasis. *Nat. Rev. Microbiol.* **8**, 481–490 (2010).
6. M. S. Tonetti, M. A. Imboden, N. P. Lang, Neutrophil migration into the gingival sulcus is associated with transepithelial gradients of interleukin-8 and ICAM-1. *J. Periodontol.* **69**, 1139–1147 (1998).
7. G. Hajishengallis, R. P. Darveau, M. A. Curtis, The keystone-pathogen hypothesis. *Nat. Rev. Microbiol.* **10**, 717–725 (2012).
8. M. A. Curtis, C. Zenobia, R. P. Darveau, The relationship of the oral microbiotia to periodontal health and disease. *Cell Host Microbe* **10**, 302–306 (2011).
9. Y. Tsukamoto *et al*., Role of the junctional epithelium in periodontal innate defense and homeostasis. *J. Periodontal Res.* **47**, 750–757 (2012).
10. C. Zenobia *et al*., Commensal bacteria-dependent select expression of CXCL2 contributes to periodontal tissue homeostasis. *Cell. Microbiol.* **15**, 1419–1426 (2013).
11. G. Hajishengallis *et al*., Low-abundance biofilm species orchestrates inflammatory periodontal disease through the commensal microbiota and complement. *Cell Host Microbe* **10**, 497–506 (2011).
12. K. Irie, C. M. Novince, R. P. Darveau, Impact of the oral commensal flora on alveolar bone homeostasis. *J. Dent. Res.* **93**, 801–806 (2014).
13. R. P. Darveau, The oral microbial consortium's interaction with the periodontal innate defense system. *DNA Cell Biol.* **28**, 389–395 (2009).
14. H. Löe, E. Theilade, S. B. Jensen, Experimental gingivitis in man. *J. Periodontol.* **36**, 177–187 (1965).
15. S. Kurgan, A. Kantarci, Molecular basis for immunohistochemical and inflammatory changes during progression of gingivitis to periodontitis. *Periodontol. 2000* **76**, 51–67 (2018).
16. C. Zemouri *et al*., Resistance and resilience to experimental gingivitis: A systematic scoping review. *BMC Oral Health* **19**, 212 (2019).
17. D. N. Tatakis, L. Trombelli, Modulation of clinical expression of plaque-induced gingivitis. I. Background review and rationale. *J. Clin. Periodontol.* **31**, 229–238 (2004).
18. L. Trombelli *et al*., Experimental gingivitis: Reproducibility of plaque accumulation and gingival inflammation parameters in selected populations during a repeat trial. *J. Clin. Periodontol.* **35**, 955–960 (2008).
19. L. Trombelli *et al*., Modulation of clinical expression of plaque-induced gingivitis. II. Identification of "high-responder" and "low-responder" subjects. *J. Clin. Periodontol.* **31**, 239–252 (2004).
20. H. Löe, J. Silness, Periodontal disease in pregnancy I. Prevalence and severity. *Acta Odontol. Scand.* **21**, 533–551 (1963).
21. J. Silness, H. Löe, Periodontal disease in pregnancy II. Correlation between oral hygiene and periodontal condition. *Acta Odontol. Scand.* **22**, 121–135 (1964).
22. S. Kurgan, A. Kantarci, Molecular basis for immunohistochemical and inflammatory changes during progression of gingivitis to periodontitis. *Periodontol. 2000* **76**, 51–67 (2018).
23. C. Genolini, X. Alacoque, M. Sentenac, C. Arnaud, kml and kml3d: R packages to cluster longitudinal data. *J. Stat. Softw.* **65**, 1–34 (2015).
24. N. C. Wellappuli *et al*., Oral and blood neutrophil activation states during experimental gingivitis. *JDR Clin. Trans. Res.* **3**, 65–75 (2018).
25. L. L. Santos *et al*., Macrophage migration inhibitory factor regulates neutrophil chemotactic responses in inflammatory arthritis in mice. *Arthritis Rheum.* **63**, 960–970 (2011).
26. L. A. Jordan *et al*., Inhibition of CCL3 abrogated precursor cell fusion and bone erosions in human osteoclast cultures and murine collagen-induced arthritis. *Rheumatology (Oxford)* **57**, 2042–2052 (2018).
27. M. Al-Sabbagh *et al*., Bone remodeling-associated salivary biomarker MIP-1α distinguishes periodontal disease from health. *J. Periodontal Res.* **47**, 389–395 (2012).
28. I. Bhavsar, C. S. Miller, M. Al-Sabbagh, "Macrophage inflammatory protein-1 alpha (MIP-1 alpha)/CCL3: As a biomarker" in *General Methods in Biomarker Research and Their Applications*, V. R. Preedy, V. B. Patel, Eds. (Springer, 2015), pp. 223–249.
29. B. J. Votta *et al*., CKbeta-8 [CCL23], a novel CC chemokine, is chemotactic for human osteoclast precursors and is expressed in bone tissues. *J. Cell. Physiol.* **183**, 196–207 (2000).
30. A. F. Stadler *et al*., Gingival crevicular fluid levels of cytokines/chemokines in chronic periodontitis: A meta-analysis. *J. Clin. Periodontol.* **43**, 727–745 (2016).
31. B. S. Mulholland, M. R. Forwood, N. A. Morrison, Monocyte chemoattractant protein-1 (MCP-1/CCL2) drives activation of bone remodelling and skeletal metastasis. *Curr. Osteoporos. Rep.* **17**, 538–547 (2019).
32. J. L. Pathak *et al*., CXCL8 and CCL20 enhance osteoclastogenesis via modulation of cytokine production by human primary osteoblasts. *PLoS One* **10**, e0131041 (2015).
33. Y. Hosokawa, I. Hosokawa, K. Ozaki, H. Nakae, T. Matsuo, CXC chemokine ligand 16 in periodontal diseases: Expression in diseased tissues and production by cytokine-stimulated human gingival fibroblasts. *Clin. Exp. Immunol.* **149**, 146–154 (2007).
34. R. Bhattacharjee *et al*., Efficacy of triphala mouth rinse (aqueous extracts) on dental plaque and gingivitis in children. *J. Investig. Clin. Dent.* **6**, 206–210 (2015).

35. J. Hwang *et al*., Human CC chemokine CCL23, a ligand for CCR1, induces endothelial cell migration and promotes angiogenesis. *Cytokine* **30**, 254–263 (2005).
36. B. J. Callahan, K. Sankaran, J. A. Fukuyama, P. J. McMurdie, S. P. Holmes, Bioconductor workflow for microbiome data analysis: From raw reads to community analyses. *F1000 Res.* **5**, 1492 (2016).
37. R. P. Darveau, A. Tanner, R. C. Page, The microbial challenge in periodontitis. *Periodontol. 2000* **14**, 12–32 (1997).
38. E. Theilade, W. H. Wright, S. B. Jensen, H. Löe, Experimental gingivitis in man. II. A longitudinal clinical and bacteriological investigation. *J. Periodontal Res.* **1**, 1–13 (1966).
39. X. He *et al*., Cultivation of a human-associated TM7 phylotype reveals a reduced genome and epibiotic parasitic lifestyle. *Proc. Natl. Acad. Sci. U.S.A.* **112**, 244–249 (2015).
40. K. Y. Zee, L. P. Samaranayake, R. Attström, An in vivo replica study of microbial colonization in "rapid" and "slow" dental plaque formers. *APMIS* **108**, 113–121 (2000).
41. G. Hajishengallis, The inflammophilic character of the periodontitis-associated microbiota. *Mol. Oral Microbiol.* **29**, 248–257 (2014).
42. E. R. Herrero *et al*., Antimicrobial effects of commensal oral species are regulated by environmental factors. *J. Dent.* **47**, 23–33 (2016).
43. J. Zhang, S. Kashket, P. Lingström, Evidence for the early onset of gingival inflammation following short-term plaque accumulation. *J. Clin. Periodontol.* **29**, 1082–1085 (2002).
44. S. Offenbacher *et al*., Changes in gingival crevicular fluid inflammatory mediator levels during the induction and resolution of experimental gingivitis in humans. *J. Clin. Periodontol.* **37**, 324–333 (2010).
45. C. Scapoli, D. N. Tatakis, E. Mamolini, L. Trombelli, Modulation of clinical expression of plaque-induced gingivitis: Interleukin-1 gene cluster polymorphisms. *J. Periodontol.* **76**, 49–56 (2005).
46. L. Trombelli *et al*., Interleukin-1 beta levels in gingival crevicular fluid and serum under naturally occurring and experimentally induced gingivitis. *J. Clin. Periodontol.* **37**, 697–704 (2010).
47. R. Deinzer, U. Weik, V. Kolb-Bachofen, A. Herforth, Comparison of experimental gingivitis with persistent gingivitis: Differences in clinical parameters and cytokine concentrations. *J. Periodontal Res.* **42**, 318–324 (2007).
48. K. H. Han *et al*., Vascular expression of the chemokine CX3CL1 promotes osteoclast recruitment and exacerbates bone resorption in an irradiated murine model. *Bone* **61**, 91–101 (2014).
49. A. Greer *et al*., Site-specific neutrophil migration and CXCL2 expression in periodontal tissue. *J. Dent. Res.* **95**, 946–952 (2016).
50. D. A. Scott, J. Krauss, Neutrophils in periodontal inflammation. *Front. Oral Biol.* **15**, 56–83 (2012).
51. B. A. Pancer *et al*., Effects of triclosan on host response and microbial biomarkers during experimental gingivitis. *J. Clin. Periodontol.* **43**, 435–444 (2016).
52. C. Nonnenmacher *et al*., Effect of age on gingival crevicular fluid concentrations of MIF and PGE2. *J. Dent. Res.* **88**, 639–643 (2009).
53. J. Bernhagen *et al*., MIF is a noncognate ligand of CXC chemokine receptors in inflammatory and atherogenic cell recruitment. *Nat. Med.* **13**, 587–596 (2007).
54. M. F. Madeira *et al*., MIF induces osteoclast differentiation and contributes to progression of periodontal disease in mice. *Microbes Infect.* **14**, 198–206 (2012).
55. K. Rajarathnam, M. Schnoor, R. M. Richardson, S. Rajagopal, How do chemokines navigate neutrophils to the target site: Dissecting the structural mechanisms and signaling pathways. *Cell. Signal.* **54**, 69–80 (2019).
56. C. F. Cao, Q. T. Smith, Crevicular fluid myeloperoxidase at healthy, gingivitis and periodontitis sites. *J. Clin. Periodontol.* **16**, 17–20 (1989).
57. J. Y. An *et al*., Rapamycin rejuvenates oral health in aging mice. *eLife* **9**, 9 (2020).
58. A. M. Chang *et al*., Toll-like receptor-2 and -4 responses regulate neutrophil infiltration into the junctional epithelium and significantly contribute to the composition of the oral microbiota. *J. Periodontol.* **90**, 1202–1212 (2019).
59. E. Bolyen *et al*., QIIME 2: Reproducible, interactive, scalable, and extensible microbiome data science. PeerJ [Preprint] (2018). https://peerj.com/preprints/27295/ (Accessed 18 June 2021).
60. B. J. Callahan *et al*., DADA2: High-resolution sample inference from Illumina amplicon data. *Nat. Methods* **13**, 581–583 (2016).
61. T. Chen *et al*., The human oral microbiome database: A web accessible resource for investigating oral microbe taxonomic and genomic information. *Database (Oxford)* **2010**, baq013 (2010).
62. F. E. Dewhirst *et al*., The human oral microbiome. *J. Bacteriol.* **192**, 5002–5017 (2010).
63. P. J. McMurdie, S. Holmes, phyloseq: An R package for reproducible interactive analysis and graphics of microbiome census data. *PLoS One* **8**, e61217 (2013).
64. C. Genolini *et al*., KmL3D: A non-parametric algorithm for clustering joint trajectories. *Comput. Methods Bioprograms Biomed.* **109**, 104–111 (2013).
65. D. Bates, M. Mächler, B. Bolker, S. Walker, Fitting linear mixed-effects models using lme4. *J. Stat. Softw.* **67**, 1–48 (2015).
66. Y. Benjamini, Y. Hochberg, Controlling the false discovery rate: A practical and powerful approach to multiple testing. *J. R. Stat. Soc. B* **57**, 289–300 (1995).
67. R. Lenth, Emmeans: Estimated marginal means, aka least-squares means. R Package Version 1 (2018). https://CRAN.R-project.org/package=emmeans. Accessed 18 June 2021.
68. S. Bamashmous, K. A. Kerns, R. P. Darveau, J. S. McLean, Human variation in gingival inflammation (HVGI) study. NCBI Sequence Read Archive (SRA). https://www.ncbi.nlm.nih.gov/bioproject/PRJNA615201. Deposited 25 March 2020.
69. S. Bamashmous *et al*., Human variation in gingival inflammation (HVGI) study. Github. https://github.com/mcleanlab/HVGI_Study. Deposited 8 July 2020.